



Cite this: *Sustainable Food Technol.*, 2026, 4, 1996

Optimization and nanoencapsulation of dandelion leaf extract for herbal tea: a comparative study of spray and freeze drying

Qudsiya Ayaz, Nadira Anjum, Sehrish Mustafa, Abdul Rouf, Imtiyaz Ahmad Zargar and Sajad Mohd Wani *

This study focuses on optimizing the brewing conditions and nanoencapsulation of dandelion tea extract (DTE) to enhance its stability and bioavailability. The most suitable brewing conditions were determined by using Response Surface Methodology (RSM) with a Box-Behnken design resulting in an extraction time of 110 min, temperature of 85.28 °C and water-to-tea ratio of 150 mL/5 g. The extracted polyphenols were nanoencapsulated using maltodextrin *via* spray and freeze-drying. The spray-dried powder exhibited higher encapsulation efficiency (88.5%) and controlled release (89.92%) compared to freeze-dried powder (83.51% and 75.76%, respectively), whereas freeze-dried powder showed higher antioxidant activity (85.87%) compared to spray-dried powder (81.35%) indicating better preservation of bioactive compounds. FTIR confirmed successful encapsulation *via* peak shifts, while SEM showed dented spray-dried nanoparticles and flaky, irregular freeze-dried nanoparticles. The findings suggest that nanoencapsulation of DTE *via* spray drying enhances stability and bioavailability compared to freeze drying, making it an ideal ingredient for herbal tea, and functional beverages.

Received 17th October 2025
Accepted 24th December 2025

DOI: 10.1039/d5fb00693g

rsc.li/susfoodtech

Sustainability spotlight

This study promotes sustainable food innovation by valorising dandelion (*Taraxacum officinale*) leaves -an underutilized wild resource from the Himalayan region into a functional herbal tea *via* nanoencapsulation. Using maltodextrin, a biodegradable plant-derived carrier, the process enhances the stability and bioavailability of natural antioxidants and polyphenols while minimizing dependence on synthetic additives. Following optimization of the brewing conditions, the extract was nanoencapsulated using spray- and freeze-drying techniques promoting the utilization of locally available plant based resources supporting the development of sustainable, nutritionally enriched functional beverages with improved environmental value.

1. Introduction

The herbal tea market has recently witnessed significant growth due to shifting consumer preferences toward health and wellness.^{1,2} Herbal teas, often called tisanes, have been appreciated in different cultures for hundreds of years due to their therapeutic benefits and stimulating flavour. Historically, herbal teas were mainly consumed for medicinal and healing properties, with each herb providing distinct therapeutic benefits. However, nowadays they have become more popular not just for health benefits but also due to the variety of flavors and enriching aromas.³

Taraxacum officinale commonly known as dandelion is a highly perishable and underutilized plant, despite its potential health benefits. Dandelion (*Taraxacum officinale*) belongs to the *Asteraceae* (sunflower) family, and grows in temperate climates. Dandelion tea is a well known herbal beverage, known for its

powerful antioxidants and anti-inflammatory and anti-cancer effects.⁴ It is rich in phytochemicals, including phenolic acids, triterpenes, coumarins, and flavonoids, all of which are thought to impart antioxidant, immune-boosting, anti-atherosclerotic, antitumor, antimicrobial and other beneficial effects. With innovation in preservation and processing methods, dandelion could become a valuable, sustainable ingredient in the beverage sector.⁵ However, to fully realize its potential, it is crucial to optimize the extraction and processing conditions to maximize the retention of bioactive compounds, particularly phenolics and flavonoids. Response Surface Methodology (RSM) is an analytical technique that uses a quadratic model to examine relationships between response variables and independent factors aiming to evaluate and optimize experimental conditions.

Instantization of tea converts traditional brewed tea into a soluble powder that dissolves quickly in hot water. Instant tea is commonly produced through extraction followed by drying, most frequently by spray drying or freeze drying, because these methods preserve key bioactive compounds while enabling convenient preparation.⁶

Division of Food Science and Technology, Sher-e-Kashmir University of Agricultural Sciences and Technology (SKUAST), Kashmir 190025, Shalimar, India. E-mail: wanisajad82@gmail.com; Tel: +91 9858445878



Spray and freeze-drying are widely utilized techniques for developing instant tea. Spray-drying is cost-effective for commercial use, while freeze-dried tea retains more aromatic compounds.⁷ Advances in encapsulation technologies such as nanoencapsulation incorporates active compounds into micro-particle matrices, regulating their controlled release and shielding them from external factors.⁸ Among the various drying methods for instant tea production, spray drying and freeze drying are the most prevalent techniques. Freeze drying is particularly effective for preserving heat-sensitive and volatile compounds due to its low-temperature, although it is associated with higher operational costs. In contrast, spray drying is more economical and easily scalable, which has led to its widespread application in nanoencapsulation.⁹ However, a systematic comparison of these techniques in terms of encapsulation efficiency, antioxidant retention, and controlled release is therefore necessary forming the basis for the present study.

Instant tea production often requires carrier agents to transform liquid extracts into stable powders. Maltodextrin is a popular choice because it is affordable, highly soluble, low in viscosity, and capable of forming films,^{8,10} which help protect sensitive phytochemicals during drying. Its ability to create a protective matrix makes it an effective wall material for maintaining the stability, dispersibility, and controlled release of polyphenols in both spray- and freeze-dried systems.^{11,12}

To our knowledge, no studies have explored nanoencapsulation technology using both spray-drying and freeze-drying for instant herbal tea production from dandelion leaves. The study aimed to optimize the brewing conditions for tea extraction using RSM with a Box-Behnken design, and to nanoencapsulate the extracted tea polyphenols with maltodextrin through spray and freeze-drying methods.

2 Materials and methods

2.1 Materials

Dandelion leaves were collected at higher altitudes in the Northern Himalayas in Kreeri baramulla with latitude: 34.17°N and longitude: 74.47°E. The samples were promptly cleaned to ensure their safety, followed by sanitization using a 100 ppm sodium hypochlorite solution for 10 minutes to reduce microbial load. After rinsing with distilled water, leaves were dehydrated for three hours in a cabinet dryer at 65 °C. An electric mill was used to grind the dry sample, which was then sieved through a 20-mesh screen, packed, and kept in an airtight container for later use.

2.1.1 Chemicals and reagents. All the chemicals and reagents were of analytical grade. 2,2-Diphenyl-1-picrylhydrazyl (DPPH), ethylenediaminetetraacetic acid (EDTA), sodium hydroxide, 2,4,6-Tris(2-pyridyl)-s-triazine (TPTZ), maltodextrin (MD), and all other reagents like ethanol, methanol, different salts and acids were procured from Hi-Media India.

2.2. Methods

2.2.1 Experimental design and dandelion tea infusion preparation. Response Surface Methodology (RSM) with the

Box-Behnken Design (BBD) was used to determine the optimal levels of three independent variables, time (*A*), temperature (*B*), and water-to-tea concentration (*C*) in order to identify the best combinations for four response variables, total phenolic content (TPC), total flavonoid content (TFC), antioxidant activity (measured by DPPH radical scavenging), and total yield. The coded values for these experimental factors and their corresponding levels are presented in Table 1. The variations in TPC, TFC, antioxidant activity (DPPH) and total yield in relation to the three variables (*A*, *B*, and *C*) were modelled using a second-order polynomial equation to optimize the brewing conditions for dandelion tea. A total of 17 experimental runs, including 3 center points, were conducted using the Box-Behnken design to optimize the operating conditions, which included extraction time ((*A*): 50–110 minutes), temperature ((*B*): 70–100 °C), and water-to-tea concentration ((*C*): 30–150 mL/5 g). The amount of water per 5 g of tea was measured in milliliters (m/5 g).

Dandelion tea infusions (DTIs) were brewed under different conditions as outlined in Table 2. Using a reflux condenser equipped with a magnetic stirrer and a temperature-sensor, heat-reflux extraction (HRE) was carried out. Five grams of dandelion tea leaves boiled in varying percentages of water were added to each DTI. Following the completion of the brewing process, the tea infusion was rapidly chilled and strained using Whatman filter No. 1. After that, the dandelion tea extracts were centrifuged for ten minutes at 5000 rpm using a Weswox WT-24BL. A rotating vacuum evaporator (Buchi Rotavapor R-80, Switzerland) was then used to concentrate the tea extracts in their best optimal state under lower pressure (mmHg) and at a temperature of no more than 35 °C. It was then stored in sealed plastic vials at –18 °C for additional examination after being dried in an oven at a temperature of no more than 27 °C.

2.3 Quantitative analysis

2.3.1 Total yield. Total yield was calculated in accordance with Yao *et al.*¹³ with minor modifications. Ultrapure water with reflux was used to boil the tea leaves. A portion of the filtrate was transferred to a Petri plate that had been previously weighed and dehydrated at 60 °C in an oven.

The following formula was used to determine the extraction yield:

$$Y(\text{mg g}^{-1}) = \frac{W_1 \times V_2}{W_2 \times V_1} \quad (1)$$

where W_1 is the dry matter weight (mg) post drying, W_2 is the tea sample weight (g), V_1 is the volume of the tea extract used to dry (mL), and V_2 is the total volume of the tea solution after

Table 1 Independent variables in the Box Behnken Design (BBD)

Process variables	Code	Variables level codes		
		–1	0	+1
Time (min)	A	50	80	110
Temperature (°C)	B	70	85	100
Water/Tea (ml)	C	30	90	150



Table 2 Design of experiment layout of rotatable CCD with three independent factors and the observed results of a response

Run	Time (min)	Temp (°C)	Water/tea (ml)	TPC (mg GAE/g)	TFC (mg QE/100 g)	DPPH (%)	Total yield (%)
1	80	85	90	74.02	63.03	63.02	23.24
2	50	70	90	64.48	56.89	51.02	20.74
3	80	85	90	70.98	65.12	59.89	22.95
4	50	100	90	75.38	65.23	68.56	19.94
5	50	85	30	65.59	57.58	58.98	18.57
6	80	85	90	72.25	61.89	62.36	24.36
7	110	100	90	75.27	65.87	66.15	29.01
8	80	70	30	63.18	58.42	59	23.78
9	110	70	90	77.67	67.12	67.98	27.25
10	80	85	90	74.12	64.56	63.21	26.6
11	80	85	90	76.36	63.11	60.01	24.02
12	110	85	30	71.58	61.55	62.23	28.69
13	80	70	150	73.57	64.63	60.12	23.11
14	50	85	150	72.48	63.98	64.69	17.89
15	110	85	150	77.78	68.01	70.25	30.25
16	80	100	150	72.59	66.45	71.25	25.69
17	80	100	30	71.12	62.23	61.09	24.31

extraction (mL). Y indicates the milligrams of soluble solids produced per gram of dry tea.

2.3.2 Total phenolic content (TPC). Total phenolic content was determined according to the method of Sansone *et al.*¹⁰ In short, in a 10 mL flask, 500 μ L of Folin-Ciocalteu reagent, 7 mL of distilled water, and 100 μ L of supernatant (or DLE) were mixed and kept at room temperature for 5 min. After adding 1.5 mL of saturated sodium carbonate, the volume was adjusted to 10 mL with distilled water and incubated in the dark for 2 hours. Absorbance was measured at 765 nm using a UV-vis spectrophotometer, and TPC was expressed as mg GAE/100 g dry basis. A gallic acid standard curve (0–0.5 mg per mL⁻¹) was prepared similarly.

2.3.3 Total flavonoid content (TFC). TFC was calculated as per the method given by Kumar and Karunakaran.¹⁴ A mixture of 1 mL of aluminium chloride in methanol, 1 mL of dandelion leaf extract, and acetic acid was diluted to 25 mL with ethanol. After 40 minutes, absorbance at 415 nm was recorded and represented as mg QE/100 g dw (quercetin equivalents).

2.4 Preparation of dandelion leaf extract (DLE) for determination of antioxidant properties

DLE was dissolved in 10 mL distilled water, mixed *via* vortexing, heated at 30 °C for 30 minutes, and centrifuged at 4000 rpm for 20 minutes, and the supernatant was collected for further analysis.¹⁵

2.4.1 Antioxidant activity by using DPPH. The method of Gerolis *et al.*¹⁶ was used to measure dandelion tea infusion's DPPH radical scavenging activity, with minor modifications. One milliliter (w/v) of liquid extract and one milliliter of a 0.2 mM DPPH solution in methanol were combined. After thorough shaking, the solution was allowed to sit at room temperature for 30 minutes in the dark. The mixture's absorbance was then measured at 517 nm. The following formula was used to calculate the extracts' radical scavenging activity as the percentage of DPPH radical inhibition.

$$\text{Inhibition Percentage (IP) \%} = \frac{(A_{\text{control}} - A_{\text{sample}})/A_{\text{control}}}{\times 100} \quad (2)$$

where A_{control} is the absorbance of the control and A_{sample} is the absorbance of the sample.

2.5 Preparation of nanoencapsulated powders

Maltodextrin DE 20 (10 g) was dissolved in 100 mL of purified water and left overnight. After adding 1% w/w of Tween 80 as a surfactant, the mixture was agitated for an hour. The wall material and dehydrated dandelion tea extract were mixed in 1 : 1 (w/v) ratios. A sonicator (QSONICA; model Q700) was used to homogenize the solution at 20 KHz for 15 minutes in order to increase the effectiveness of encapsulation and reduce the size of the particles to the nanoscale. The solution was then dehydrated using lyophilisation and spray drying methods.¹⁰

A Mini Spray Dryer (BUCHI, B-290), Switzerland, was used to dry the nanoemulsion. The inlet temperature of the spray dryer was set at 120 °C, with a hot air flow velocity of 2.5 m³ min⁻¹ and a peristaltic pump flow rate of 5 cm³ min⁻¹ at 0.06 MPa. The outlet temperature stabilized at approximately 68 °C. The resultant encapsulation products were gathered and kept in an airtight container for further analysis.

Freeze drying involved freezing the nanoemulsion at –20 °C and then drying it using a lyophilization system (BUCHI, Lyo-vapor L-200, Switzerland). For 48 hours, the ice condenser's temperature was kept at –56 °C, and the vacuum was adjusted to 0.074 Mbar. After 48 hours of drying, the powder was placed in sealed bags for further examination.

2.6 Physical properties of nanoencapsulated powders

2.6.1 Moisture content and water activity. The moisture content of the nanoparticles was determined at 105 °C in a hot air oven which was previously preheated. The powder's



moisture content was calculated using eqn (1). Triplicate measurements were carried out.¹⁷

$$\text{Moisture content(\%)} = \frac{\text{Weight loss(g)}}{\text{Weight of the sample}} \times 100 \quad (3)$$

A water activity measurement device from the Aqualab (Model 3 TE) series was used to measure the water's activity.

2.6.2 Bulk density (ρ_B). A 2 g portion of powder was carefully introduced into a 10 mL graduated cylinder. The bulk density was calculated by dividing the powder's weight by the volume it occupied in the cylinder.¹⁸

2.6.3 Tapped density (ρ_T). Tapped density was measured by following the standard procedure of Jinapong *et al.*¹⁸ 5 g of the sample was placed in a graduated cylinder and subjected to repeated tapping until a constant volume was obtained. The recorded sample was based on triplicate measurements.

2.6.4 Particle density (ρ_P). 5 mL of petroleum ether was added to a measuring cylinder, to which 1 g of powder was added and shaken for 1 min to obtain an even suspension. The cylinder walls were then rinsed with an extra 1 mL of petroleum ether. The 6 mL total volume containing suspended particles was measured and the density of the particles was calculated according to eqn (4).

$$\text{Particle density} = \frac{\text{Weight of powder(g)}}{\text{Total volume of petroleum ether with suspended powder(mL)}^{-6}} \quad (4)$$

The powder samples' porosity was calculated using the relationship between tapped and particle densities, as shown in eqn 5

$$\varepsilon = \frac{\rho_{\text{particle}} - \rho_{\text{tapped}}}{\rho_{\text{particle}}} \times 100 \quad (5)$$

2.6.5 Hygroscopicity. Hygroscopicity was determined employing a procedure suggested by Zokti *et al.*¹⁹ with a few modifications. Each powder sample, weighing about 1 g, was put in triplicate into vials and was stored with saturated NaCl and weighed after a week, and hygroscopicity was measured as retained moisture.

2.6.6 Flowability and cohesiveness. Nanoencapsulated powder flow properties were assessed using Carr's Index (CI) and the Hausner Ratio (HR), which calculate flow characteristics based on bulk and tapped densities. The CI values provide a classification scale ranging from very good to very poor flow

behavior, with thresholds indicating increasingly problematic flowability.

$$\text{Hausner's ratio} = \frac{\text{Tapped density}}{\text{Bulk density}} \quad (6)$$

$$\text{Carr's index(\%)} = \frac{\text{Tapped density} - \text{Bulk density}}{\text{Tapped density}} \times 100 \quad (7)$$

2.6.7 Product yield. Product yield is the proportion of the solid substance retrieved upon drying in comparison to the initial amount of solid substance consumed.²⁰ eqn (6) is used to calculate the yield.

$$\text{Product yield} = \frac{\text{Final mass of dried powder(g)}}{\text{Initial mass of solid material(g)}} \times 100 \quad (8)$$

2.6.8 Encapsulation efficiency (EE). A modified technique from Saikia *et al.*²¹ was used to measure the phenolic content in order to quantify the encapsulation efficiency (EE). For the assessment of surface polyphenols, a 200 mg sample of nano-encapsulates was diluted in 2 mL of ethanol:methanol (1:1) and filtered. An additional 200 mg of entrapped polyphenols were dissolved in a 50:8:42 mixture of methanol, acetic acid, and water, vortexed, and ultrasonically sonicated. Following

centrifugation, the supernatant was filtered, and the Folin-Ciocalteu reagent reducing capacity test was used to measure the total amount of polyphenols. The following equation was used to calculate the EE:

$$\text{EE(\%)} = \frac{\text{Total polyphenol content} - \text{Polyphenol content on surface}}{\text{Total polyphenol content}} \times 100 \quad (9)$$

2.6.9 Antioxidant capacity. The antioxidant capacity was calculated according to methods described by Filippou *et al.*²² About 1 g of powder was added to 20 mL of water and the total phenolic content and antioxidant activity were determined using the following equation:

$$\text{Antioxidant Capacity(\%)} = \frac{A_{\text{DPPH}} - A_s}{A_{\text{DPPH}}} \quad (10)$$

where A_{DPPH} is the absorbance of the blank sample and A_s is the absorbance of the sample.

For IC₅₀ determination, antioxidant capacity was evaluated at multiple sample concentrations, and the IC₅₀ value was



calculated as the concentration required for reaching 50% antioxidant capacity.

2.7 Characterization of nanoencapsulated powders

2.7.1 Particle size, polydispersity and zeta potential. Using a dynamic light scattering setup (DLS, Anton Paar, Litesizer 500) at 25 °C, the particle size of freeze-dried and spray-dried nanoparticles was measured as per the method outlined by Sanna *et al.*,²³ with minor modifications. In order to eradicate numerous scattering effects, powders were dissolved 100-fold in distilled water before testing. The particle size was checked throughout every experiment until the subsequent values were constant after a small portion of the sample was dispersed in 0.1 mM KCl. Every test was conducted at 25 °C, and the mean of all three readings were noted.

2.7.2 Functional group characterization using fourier transform infrared (FTIR) spectroscopy. FTIR (Spectrum Two, PerkinElmer) was used to characterize spray and freeze-dried nanoparticles in order to examine the bonding configuration and chemical compounds. The range of wavelengths used was 4000 cm⁻¹ to 400 cm⁻¹, with a 4 cm⁻¹ resolution and 64 scan average, and dried nanoparticles were analyzed against wall material and dandelion tea extract spectra. FTIR analyses were performed in triplicate, and representative spectra were selected from these replicates to maintain analytical consistency.

2.7.3 Scanning electron microscopy (SEM). The surface morphology of spray- and freeze-dried nanoparticles was analyzed using a field emission scanning electron microscope (FE-SEM) (Gemini SEM 500, ZEISS, Germany). Samples were examined at 1.00 k × magnification (10 μm scale) and 300 g samples at 100 μm scale, with a 5 kV accelerating voltage. Powders were affixed to aluminum strips with carbon tape. Before scanning, samples were coated with a thin gold layer (10 nm) to improve conductivity and prevent charging under the electron beam. SEM analyses were performed in triplicate, and representative images were selected from these replicates to ensure reproducibility.

2.7.4 In vitro release profile analysis and release modelling. The release of phenolic compounds from nanoencapsulated dandelion leaf extract (DLE) was evaluated using the *in vitro* digestion model under simulated gastrointestinal conditions by Rashid *et al.*,²⁴ with slight modifications. A model of the simulated gastrointestinal tract was used to digest 300 mg of nano-capsules. Samples were mixed with 15 mL of simulated gastric juice which was prepared by mixing 3 g per L of pepsin with 9 g per L saline, and pH was adjusted to 2 by using 1 M HCl during the gastric phase. They were then incubated for three hours at 37 °C in an orbital shaker (8 × g). During this phase, periodically, 2 mL aliquots were taken out from the whole mixture, chilled, and kept at -20 °C. After three hours, the gastric phase was completed, and the mixture was centrifuged. The combination was centrifuged once the gastric phase was finished, and the pellets that were produced were employed to mimic intestine digestion. The pellets were reconstituted in 15 milliliters of simulated intestinal juice (SIJ), which was made by dissolving

10 g per L pancreatin and 3 g per L bile salts in phosphate buffer (pH 7.5). After that, the mixture was incubated for four hours at 37 °C, and 2 mL aliquots were collected from the whole reconstituted mixture every 60 minutes. This approach ensures that aliquots represent the complete sample at each stage before centrifugation, and the separation of the pellet post-gastric phase allowed for proper simulation of intestinal digestion. To examine the release mechanism of dandelion tea extract from nanoencapsulates in gastrointestinal media, data from *in vitro* release studies were determined employing a range of mathematical models, such as the Korsmeyer, Higuchi, Hixson-Crowwell, zero order, and first order models²⁵ to determine the most appropriate model. To assess these models' suitability for delivery profiles, the determination coefficient (R^2) was employed.

2.7.5 Statistical analysis. Every experiment was performed in triplicate, and the mean ± standard deviation was used to determine the results. One-way analysis of variance (ANOVA) was used using Tukey's HSD (honestly significant difference) test at a significance level of $p \leq 0.05$. All values were obtained in triplicate, and the results were expressed as mean ± standard deviation (SD). The response surface methodology (RSM) with Box-Behnken Design was used to optimize the experiment. The Statistical Software Design Expert 12 (Stat-Ease Inc., Minneapolis, MN, USA) was used for model fitting and optimization, while OriginPro 9.0 was used for generating all graphical outputs.

3. Results and discussion

3.1. Fitting of the model

The analysis of variance (ANOVA) presented in Table 3 indicates that independent factors have a substantial ($p < 0.05$) effect on the models developed for every response. All the selected parameters had extremely significant coefficients of determination (R^2), which ranged from 0.9052 to 0.9590, suggesting the adequate fit of mathematical models with real data. Predicted R^2 and adjusted R^2 were found to be reasonably in agreement for all significant models. Additionally, for every model, the precision and coefficient of variation fell between 12.339 and 17.859 and 1.77 and 5.04% respectively, confirming the accuracy, dependability, and reproducibility of the results, as shown in Table 3. Lack of fit for all the models was found to be non-significant, validating their close fit with the observed data. Additionally, the adequate precision was more than 4 for all the models, which guarantees high reliability and is appropriate for validation.

3.2 Effect of independent variables (extraction parameters) on dependent variables of dandelion tea

3.2.1 Total phenolic content (TPC). Total phenolic content went from 63.18 to 77.78 (mg GAE/g) as shown in Table 2. A second degree model depicting the TPC content is given below in eqn (11), which specifies the significant ($p < 0.05$) positive linear effects of *A* and *B* respectively as shown below:



Table 3 Results of the ANOVA for the fit of the data to the response surface model

Responses	R^2	Predicted R^2	Adjusted R^2	Regression adequate precision	C.V.	p -value	Lack of fit
Total phenolic content	0.9402	0.8631	0.8633	12.3395	2.20	<0.0017	0.9727
Total flavonoid content	0.9480	0.7440	0.8812	12.4092	1.77	<0.0010	0.7584
DPPH	0.9590	0.7304	0.9064	16.9682	2.42	<0.0005	0.5944
Total yield	0.9052	0.8412	0.8833	17.8592	5.04	<0.0001	0.7687

$$\text{TPC} = 73.55 + 3.05A + 1.93B + 3.12C - 2.39C^2 \quad (11)$$

where A represents extraction time, B denotes extraction temperature, and C signifies the water-to-tea ratio. The positive values of the linear terms A , B , and C indicate that increasing extraction time, temperature and water: tea ratio had a greater influence on the TPC of dandelion tea. As both the extraction time and temperature increased, more phenolic compounds are extracted, increasing the phenolic compounds' solubility and rate of diffusion.²⁶ Our results align with those of Parvez *et al.*,²⁷ who found that increasing extraction temperatures and times led to higher TPC. Additionally, water's dielectric constant decreases with increasing temperature, lowering hydrogen bonding and improving its solvent properties for nonpolar phenolic chemicals.²⁸ This increases solubility, which in our study improves the extraction efficiency of phenolics at higher temperatures. Furthermore, the liquid to solid ratio increased with more increase in the total phenolic content which might be attributed to increased solvent volume, which improves penetration into the cells and facilitates more effective phenolic compound leaching and extraction.²⁹ However, the negative quadratic effect of the water to tea ratio indicates that beyond a certain point, further increases in the ratio could reduce the phenolic content resulting in decreased extraction efficiency. Similar reports were obtained by Parvez *et al.*²⁷

3.2.2 Total flavonoid content (TFC). TFC ranged between 56.89 and 68.01 mg QE/100 g as shown in Table 2. The regression eqn (12) obtained for TFC is given below.

$$\text{TFC} = 63.54 + 23.6A + 1.59B + 2.91C - 2.40AB \quad (12)$$

where A : time, B : temperature and C is the water: tea ratio.

From eqn (12), it was observed that the independent variables *i.e.* extraction time, (A) extraction temperature (B) and water: tea ratio (C), had a positive significant ($p < 0.05$) effect on TFC. The total flavonoid content increases with increasing extraction time and temperature. This could be because tea leaves are easier to penetrate, which increases their surface area for interaction with water and facilitates a higher level of flavonoid extraction throughout. Additionally, a longer extraction period allows for the dissolution of more flavonoids.³⁰ Wang *et al.*³¹ noted similar findings on the optimization of brewing conditions for vine tea. Additionally, it was shown that a larger water to solid ratio enhanced the TFC. This behaviour is most likely caused by a larger volume of solvent, which speeds up compound diffusion by effectively dissolving flavonoids and extracting more solid materials from cells, improving the

extraction process and overall enhancing the TFC.³² Insang *et al.*³³ noted similar findings during the mulberry leaf extraction process. Moreover, the interactive effect between extraction time and temperature (AB) revealed a significant negative impact ($p < 0.05$) on TFC.

3.2.3 Antioxidant activity measured by using DPPH. The DPPH score ranged from 51.02% to 71.25% as shown in Table 2. The significant ($p < 0.05$) predicted model obtained for DPPH from regression analysis is given in eqn (13) provided below:

$$\text{DPPH} = 61.70 + 2.92A + 3.62B + 3.13C - 4.84AB \quad (13)$$

where A is the extraction time, B is the extraction temperature, and C is the water: tea ratio.

The fitted model shows that all three independent variables have a substantial ($p < 0.05$) positive linear impact on DPPH. DPPH increased when A , B , and C increased, based on the positive values of linear components of extraction time (A), extraction temperature (B), and solid liquid ratio (C). The reason for this could be due to the higher temperatures which speed up the extraction process and make antioxidants more soluble and easier to release from the tea leaves; increasing both time and temperature boosts the overall antioxidant activity. In contrast to less stable, less soluble antioxidants, heat-stable antioxidants in particular are less likely to degrade at higher temperatures, enabling a faster extraction rate.³⁴ Similar outcomes were noted by Lee *et al.*³⁵ Furthermore, the antioxidant activity increased when the water-to-solid ratio increased as shown in Table 4 This might be because of the larger volume of the solvent, which increases the possibility that antioxidants will come into contact with the extraction solvent and help move bioactive chemicals into the liquid phase.²⁹ Wati *et al.*³⁶ also noted a similar pattern. Moreover, tea's antioxidant activity was significantly ($p < 0.05$) impacted negatively by the interaction of extraction time (A) and temperature (B).

3.2.4 Total yield. Total yield (TY) ranged between 17.89 and 30.25% as shown in Table 2. Eqn (14) below provides the significant ($p < 0.05$) predicted model for TY derived from regression analysis.

$$\text{TY} = 24.14 + 4.76A \quad (14)$$

where A is the extraction time.

From the regression eqn (14), TY increased significantly ($p < 0.05$) as extraction time (A) increased. This could be explained by the fact that longer extraction times improve the extraction of more antioxidant substances as well as tea polyphenols, allowing more bioactive substances to be discharged into the liquid



Table 4 Comparison of predicted and actual responses

Values	Total phenolic content (mg GAE/g)	Total flavonoid content (mg QE/100 g)	DPPH (%)	Total yield (%)
Predicted values	77.78	68.04	70.68	29.10
Actual values	76.58	67.12	69.88	28.28
Variation (%)	1.54	1.35	1.13	2.81

medium and enhancing the proportion of total yield.³⁷ Similar findings regarding the Hirsute leaf extraction technique were noted by Pham *et al.*³⁸

3.3 Validation of the model and optimization

The optimal conditions were determined using the desirability function approach, yielding a desirability score of 0.969 (Fig. 1). The best conditions for making dandelion tea were determined to be 110 minutes extraction time, 85.28 °C extraction temperature, and 150.00 mL/5 g water-to-tea ratio. The predicted and experimentally obtained values for responses were 77.78 and

76.68 mg GAE/g for TPC, 68.04 and 67.12 mg QE/g for TFC, 70.68 and 69.88% for DPPH antioxidant activity, and 29.10 and 28.28% for total yield respectively. A strong connection between the predicted and experimental results confirmed the validity of the current RSM model. The experimental results closely matched the predicted response values, with a difference of less than 4%.

3.4 Physical characteristics of nanoencapsulated powders

3.4.1 Moisture content and water activity. Moisture content (MC) and water activity (*a_w*) are significant variables

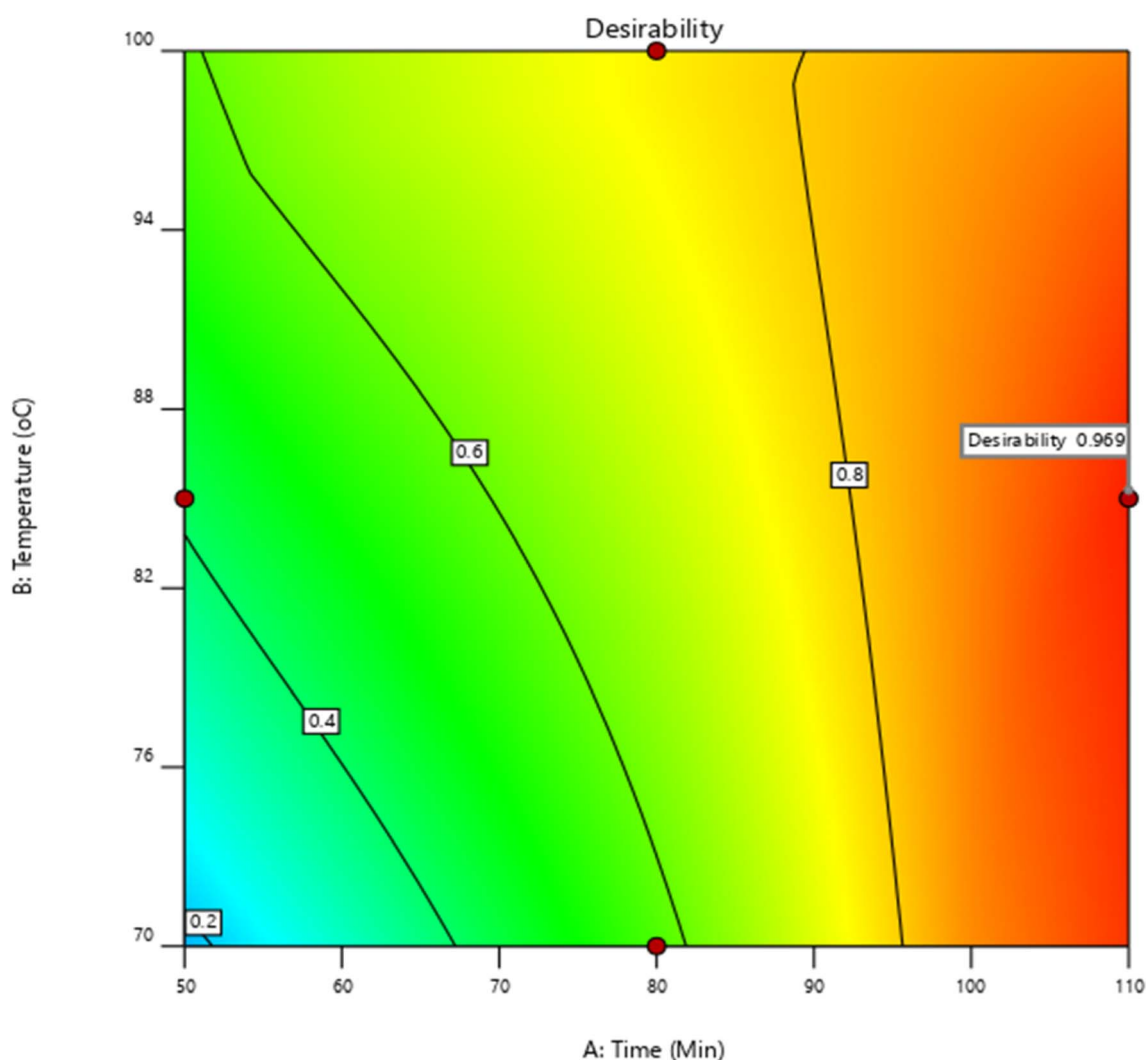


Fig. 1 Response surface plot showing the desirability function.



Table 5 Physical properties and flow characteristics of nano-encapsulate powders^a

Parameters	Freeze dried	Spray dried
Moisture content (%)	3.49 ± 0.31 ^a	2.69 ± 0.42 ^b
Water activity (aw)	0.29 ± 0.02 ^a	0.2 ± 0.02 ^b
Bulk density (g cm ⁻³)	0.42 ± 0.02 ^b	0.59 ± 0.03 ^a
Tapped density (g cm ⁻³)	0.46 ± 0.03 ^b	0.71 ± 0.01 ^a
Particle density (g cm ⁻³)	1.48 ± 0.04 ^b	1.65 ± 0.02 ^a
Hygroscopicity (%)	12.25 ± 0.07 ^b	14.59 ± 0.09 ^a
Porosity (%)	68.91 ± 1.63 ^a	57.57 ± 1.63 ^b
Carr's index (flowability)	8.69 ± 0.04 ^b	17.14 ± 0.04 ^a
Hausner ratio (cohesiveness)	1.09 ± 0.01 ^b	1.20 ± 0.01 ^a

^a All values are reported as mean ± standard deviation from three replicates. Statistically significant differences ($p \leq 0.05$) between the freeze-dried and spray-dried encapsulates within rows are represented by different lowercase letters (a and b).

that affect the adhesion, permeability, and quality of powders during storage.³⁹ The shelf life of powders is significantly influenced by both MC and aw. The results for water activity and moisture content in both spray and freeze-dried tea powders, presented in Table 5 showed significant differences ($p < 0.05$). Higher MC and aw were observed in freeze dried powders with values of 3.49% and 0.29, while the spray dried powder had a lower moisture content of 2.69% and aw of 0.20 respectively. The reason for the lower MC and aw may be attributed to the high temperature of the spray drying process and the smaller droplet size, which resulted in an increased rate of mass transfer. This enlarged surface area enables water molecules to migrate more rapidly from the droplet interior to the surface. As these droplets are exposed to the high inlet air temperature, a large temperature gradient is created between the droplet surface and the drying air. This gradient accelerates the evaporation rate, leading to immediate removal of moisture.⁴⁰ A similar trend was observed by Kuck and Norena⁴¹ for phenols encapsulated from grape skins. Overall, aw of both the samples fell within the standard range for powdered samples and met within the recommended threshold for microbial stability (<0.6).

3.4.2 Bulk density, tapped density and particle density.

Bulk density and tapped density are crucial parameters for evaluating the convenience of handling, storing, packaging, and transportation of powdered food items. Table 5 shows that the bulk and tapped density values of powdered materials differed significantly ($p < 0.05$). The bulk and tapped densities of the freeze-dried encapsulates were 0.42 and 0.46 g cm⁻³, whereas the spray-dried encapsulates exhibited a density of 0.59 and 0.71 g cm⁻³, respectively. Spray dried samples exhibited higher density in comparison to freeze dried samples. The shape and surface characteristics of the particles are responsible for the greater bulk and tapped densities in the spray dried tea samples. Moreover, the spherical, homogeneous, compact, and smaller sized spray-dried particles result in a larger mass per unit volume and thus, a higher bulk density. Conversely, the irregular shape of the freeze-dried particles enables water to be removed, creating hollow regions which increase the total

volume and decrease the bulk density.⁴² These findings align with those reported by Dadi *et al.*⁴³. Furthermore, the tapped density exceeded the bulk density as tapping enabled smaller particles to fill gaps between larger ones, creating a denser structure.⁴⁴

Particle density is a significant variable for estimating the true density of particulates, eliminating the void regions among them. The particle densities of both powders differed significantly ($p < 0.05$) as shown in Table 5. The spray-dried sample had a higher particle density of 1.65 g cm⁻³, while the freeze-dried sample showed a lower particle density of 1.48 g cm⁻³. The difference in powdered density between the spray-dried and freeze-dried samples may be the reason for the higher particle density in the former. Less air space between the particles makes higher bulk density powders ideal for storing. During spray drying, compact, spherical particles are formed as a result of rapid evaporation of water due to high temperature which leads to smaller sizes and greater uniformity; these particles pack more tightly, hence increasing the particle density. In addition, a higher bulk density can result in superior flow characteristics, lower settling down, and less vulnerability to moisture absorption, all of which enhance performance and extend shelf life in a variety of applications.⁴⁵ Our findings are consistent with the outcomes of Bashir *et al.*⁴⁶

3.4.3 Hygroscopicity and porosity. The capacity of an encapsulated bioactive substance to absorb moisture from its surroundings is reflected in its hygroscopicity, which is an important consideration. It is usually represented as the amount of water retained per 100 grams of the sample, and can influence the durability of the product.⁴³ The hygroscopicity of both the powders showed significant differences ($p < 0.05$), as indicated in Table 5. The hygroscopicity of spray-dried samples was 14.59%, whereas that of freeze-dried samples was 12.25%. Compared to the freeze-dried nanoencapsulates, the spray-dried ones showed noticeably greater hygroscopicity. This difference is likely due to the lower moisture content of the spray-dried nanocapsulates, which leaves more unoccupied active sites on the particle surface; these exposed sites readily attract and bind water vapour from the surrounding environment, ultimately leading to higher hygroscopicity. According to Tonon *et al.*,⁴⁷ it is widely observed that particles with reduced moisture content have a better ability to retain moisture from surrounding air and, as a result, exhibit increased hygroscopicity. The findings are further supported by Shuen *et al.*,¹⁷ who found that spray-dried kuini powdered samples had increased hygroscopicity.

Porosity is a crucial component of powder reconstitution and represents an additional important feature in food processing. Since porosity quantifies the percentage of total volume occupied by void spaces, it is related to bulk density.⁴⁵ A statistically significant difference ($p \leq 0.05$) was observed in the porosity of both powders with spray dried tea powder having a porosity of 57.57% and freeze-dried tea powder showing a porosity of 68.91% as given in Table 5. Lower porosity was exhibited by spray dried powder while higher porosity was shown by freeze dried powder. The reason for lower porosity might be due to the higher bulk density and particle arrangement of the spray-dried



nano-encapsulated samples. Because of their smaller size, the particles are packed closer together, creating fewer spaces between them and reducing the material's porosity compared to the freeze-dried powder. Additionally, the lower bulk density values of the freeze-dried powder samples can be explained by their higher porosity, which resulted from phase transition of ice that creates voids, thereby increasing the product's porosity.⁴⁸ Previous studies by Karam *et al.*,⁴⁹ revealed the same outcomes with freeze-dried and spray-dried mango powders.

3.4.4 Flowability and cohesiveness. The Hausner ratio (HR) and Carr index (CI) evaluated the nanoencapsulated powder's flow properties and cohesiveness. These indices classify powder characteristics from extremely poor to excellent flowability and cohesive behavior, as established by Muzaffar *et al.*⁵⁰

The powder's bulk and tapped densities are used to calculate the CI and HR values. Greater cohesion and poor flowability are indicated by higher values of the Hausner Ratio (HR) and Carrs Index (CI). Table 5 indicates that the CI and HR values for freeze-dried tea powder varied between 8.69 and 1.09, while the values for spray-dried tea powder were 17.14 and 1.20, respectively. In contrast to the freeze-dried powder, which showed greater flowability and lower cohesiveness, the spray-dried powder had higher HR and CI values, suggesting that the substance is more cohesive and has poor flowability. This might be because of the low moisture content, which has been demonstrated to improve powder particle cohesiveness and decrease flowability.⁵¹ Furthermore, the homogeneity and fine particle size in the freeze-dried powder sample decreased interstitial spaces, maximizing surface availability in contact with the surrounding air. This consequently results in lower values for the Hausner Ratio and Carr Index in freeze-dried powder,⁵² and our findings correlate with those of Caliskan and Dirim.⁵³

3.4.5 Product yield. The product's yield is a key indicator that reflects the effectiveness of the drying process employed and has an enormous effect on the price. The yield of tea powders encapsulated using freeze-drying and spray-drying methods is shown in Table 6. The yield of the two types of powders differed significantly ($p < 0.05$), with the spray-dried powder showing a yield of 76.3% and the freeze-dried powder

showing a yield of 85.7%. The poorer yield of the spray-dried powder can be explained by the higher temperatures and atomization used during the process.⁵⁴ These conditions enhance heat and mass transfer, which in turn increases the glass transition temperature (T_g) of the amorphous components, leading to greater particle loss. Furthermore, this effect can lead to increased moisture loss and decreased yield.⁵⁵ In contrast, the lower temperatures used in freeze-drying probably result in a better recovery due to a decrease in the powder's tendency to adhere to the chamber walls. Moreover, freeze-drying improves yield by maintaining the structure and reduces the loss of volatile ingredients. Shuen *et al.*¹⁷ reported a higher product yield for the freeze-dried powder of kuini pulp powder, which is in line with our findings. Xin *et al.*⁵⁶ also reported similar outcomes in their comparison of freeze- and spray-dried flavouring powders, noting that freeze-dried samples consistently exhibited higher product yields than spray-dried samples.

3.4.6 Encapsulation efficiency (EE). Encapsulation efficiency (EE) is a crucial factor, since it measures the ability of the encapsulating substance to hold its main component within its structure and demonstrates the efficiency of the method of encapsulation. Table 6 illustrates the EE of the freeze dried and spray-dried powders. A significant difference ($p < 0.05$) was observed in the encapsulation efficiencies of both powders. Spray drying demonstrated a higher encapsulation efficiency (EE) of 88.5%, compared to freeze drying, which had an EE of 83.51%. Greater retention of volatile compounds throughout the drying process reflects the difference in encapsulation efficiency. According to this, spray drying makes it easier for nanocapsules to develop inside the film-forming shell later on in the drying process, which improves extract entrapment and reduces surface content.⁵⁵ Conversely, freeze drying promotes droplet-to-droplet interactions inside the emulsion. This extended drying period causes the extract to be inconsistently entrapped, which lowers the entrapment effectiveness and increases the surface content. These results suggest that spray drying provides superior encapsulation stability compared to freeze drying. Junior *et al.*⁵⁷ noted similar observations while evaluating the drying of ciriguela peel using spray and freeze-drying techniques. Furthermore, the spherical morphology typically formed during spray drying also contributes to improved encapsulation efficiency, which explains the higher EE observed in the spray-dried powder compared to the freeze-dried powder. Similar findings were reported by Bashir *et al.*⁴⁶ who noted higher encapsulation efficiency for spray-dried vitamin D nanoparticles relative to those obtained by freeze drying.

3.4.7 Antioxidant capacity. Antioxidant capacity refers to the ability of a compound or extract to neutralize free radicals and prevent oxidative damage. Table 6 presents the antioxidant capacity of the freeze-dried and spray-dried powders. A significant difference ($p < 0.05$) was observed in the antioxidant capacities of the two powders. The freeze-dried powder exhibited a higher antioxidant capacity of 85.87%, whereas the spray-dried powder showed a slightly lower value of 81.35%. Lower antioxidant capacity in spray dried powder might be due to the

Table 6 Product yield, encapsulation efficiency, antioxidant capacity, particle size, polydispersity index and zeta potential of nano-encapsulated powder^a

Parameters	Freeze dried	Spray dried
Product yield (%)	85.29 ± 1.51 ^a	75.96 ± 1.31 ^b
Encapsulation efficiency (%)	83.51 ± 0.77 ^b	88.5 ± 0.94 ^a
Antioxidant capacity (%)	85.87 ± 1.53 ^a	81.35 ± 0.67 ^b
IC ₅₀ (mg mL ⁻¹)	1.71 ± 0.03 ^a	1.94 ± 0.06 ^b
Particle size (nm)	290.26 ± 2.36 ^a	180.45 ± 1.54 ^b
Polydispersity index	0.29 ± 0.02 ^b	0.34 ± 0.02 ^a
Zeta potential (mv)	-24.4 ± 0.63 ^b	-20.5 ± 1.37 ^a

^a All values are expressed as mean ± standard deviation from three replicates. Statistically significant differences ($p \leq 0.05$) between the freeze-dried and spray-dried encapsulates within each row are denoted by different lowercase letters (a and b).



rapid droplet atomization and solvent evaporation in the spray drying process which promotes early formation of a continuous carrier film around the core material, producing compact, spherical particles with reduced surface polyphenol exposure and antioxidant activity of powders, suggesting a potential loss or antioxidant activity during the drying process.⁵⁸ In contrast, freeze drying generally preserves higher antioxidant activity, which can be attributed to its low-temperature and vacuum-based process which minimizes thermal degradation, oxidation, and structural collapse of heat-sensitive phytochemicals thereby retaining more bioactive compounds. Similar findings were reported in the study by Varelzic *et al.*^{59,60} who compared the antioxidant potential of spray-dried and freeze-dried extracts obtained from oregano processing wastes using an optimized ultrasound-assisted extraction method.

The IC₅₀ values derived from antioxidant capacity measurements indicate that the freeze-dried powder exhibited slightly higher antioxidant potency, as reflected by its lower IC₅₀ value (1.71 mg mL⁻¹) compared with the spray-dried powder (1.94 mg mL⁻¹). This outcome reflects the advantage of low-temperature processing in preserving phenolic antioxidants. Similar trends were reported by Liang *et al.*⁶¹ for *Spiranthes sinensis*, where minimally heated extracts showed lower IC₅₀ values. Turkiewicz *et al.*⁶² also observed higher IC₅₀ values in spray dried medicinal-plant extracts.

3.5 Characterization of encapsulated powders

3.5.1 Particle size, PDI and zeta potential

3.5.1.1 Particle size. Particle size plays a key role in determining stability, encapsulation efficiency, and the overall accessibility of the core substance. It's crucial for enhancing targeted nutrition and medicinal applications, ensuring the effectiveness of the product. Table 6 depicts the particle size of the tea powder nanoparticles that were encapsulated using freeze and spray drying. The freeze-dried tea samples exhibited a larger particle size of 290.26 nm, while the spray dried powder samples had a particle size of 180.45 nm. The reduction in the particle size of the spray-dried sample may be due to the high inlet temperature and atomization.⁶³ Moreover, the larger size of the particles in freeze drying can be attributed to the agglomeration of particles during the formation of ice crystals due to the lower temperature used in the process and the inability of forces to break the frozen medium into tiny droplets. Our results are in line with Chen *et al.*⁶⁴ for spray and freeze drying of water pea.

3.5.1.2 Polydispersity index (PDI). The polydispersity index (PDI) is essential for evaluating uniformity and stability of the particle size dispersion. The distribution of particle size is measured by the PDI value, which is greater for samples exhibiting greater size diversity than for samples with uniformly sized particles.⁶⁵ Furthermore, a polydispersity index below 0.4 suggests a narrow particle size distribution.⁶⁶ Table 6 presents the PDI values for the freeze dried and spray dried powders and were recorded as 0.29 and 0.34 respectively. The freeze-dried samples exhibited a lower PDI, whereas the spray dried samples showed a higher PDI. This is because in freeze drying,

each sample is frozen separately and then dried at low temperatures and pressures, which might cause cell rupture and enhance the capsule's internal environment that promotes the production of smaller particles. However, spray drying can result in particle aggregation and produces larger particles by spraying the liquid sample and drying it at high temperatures.⁶⁷ Consequently, the polydispersity index (PDI) will probably be more uniform in freeze drying. Our results for the polydispersity index (PDI) are consistent with those of Ma *et al.*,⁵² who compared freeze-drying (FD) and spray-drying (SD) in stable silybin nanosuspensions.

3.5.1.3 Zeta potential. Zeta-potential plays a vital role in evaluating how stable a colloidal system is. It is an essential component in estimating the degree of stability of microparticles and serves as an indicator of net surface charge. The stability of nanoparticles is generally determined by their charge. A zeta potential exceeding +30 mV or falling below -30 mV indicates an ideal condition for maintaining long-term colloidal stability. In general, the z-potential can be used to calculate the extent of both stability and instability of suspensions. The probability of particle aggregation due to electric repulsion decreases with increasing z-potential.⁶⁸ From Table 6, the zeta potentials of the freeze-dried and spray-dried tea powders were -24.4 mV and -20.5 mV, respectively. The lower zeta potential in freeze-dried samples is primarily due to an increase in particle size which decreases the surface area available for charge dispersion and electrostatic repulsion.⁶⁹ Comparable observations were reported by Ledari *et al.*,⁷⁰ when they assessed two drying methods for chlorophyll encapsulation.

3.5.2 Fourier transform infrared (FTIR) spectroscopy. The FT-IR method identifies the molecular composition and chemical bond properties of various components and therefore can be utilized to examine the molecular interactions between the active substance and the encapsulating agent.⁷¹ Fig. 2 shows

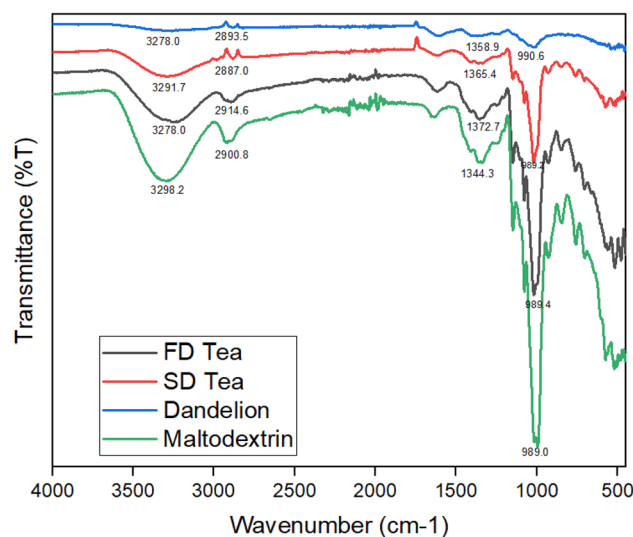


Fig. 2 FTIR spectra of maltodextrin, dandelion tea, spray dried tea powder (SD) and freeze dried tea powder.



the FT-IR spectra of dandelion powder and carrier material (maltodextrin) spray-dried and freeze-dried tea powder across the wavelength range of 4000–500 cm^{-1} . The FT-IR spectra displayed similar functional group peak characteristics, consistent with the findings from previous research.⁷² The FTIR spectra of tea extract, maltodextrin, and encapsulated tea extract (both freeze-dried and spray-dried) in our study revealed characteristic peaks that indicate interactions between the active components of tea extract and the maltodextrin carrier, as well as subtle shifts due to the encapsulation process. The broad O–H stretching band appeared at 3298.2 cm^{-1} in maltodextrin and 3278.0 cm^{-1} in dandelion extract. After encapsulation, this band was detected at 3278.0 cm^{-1} in the freeze-dried (FD) powder and shifted to 3291.7 cm^{-1} in the spray-dried (SD) powder. This upward shift towards higher wavenumbers in SD is attributed to the hydroxyl groups (–OH) in polyphenolic compounds like catechins and the carrier matrix, indicating a modified hydrogen-bonding environment caused by rapid moisture evaporation and higher thermal exposure. Similarly, the asymmetric C–H stretching region displayed notable variations; maltodextrin exhibited a peak at 2900.8 cm^{-1} , whereas the encapsulated powders showed peaks at 2914.6 cm^{-1} (FD) and 2887.0 cm^{-1} (SD), reflecting structural adjustments and differences in molecular packing. The carbonyl (C=O) stretching region characteristic of carbohydrates showed distinct movement, shifting from 1358.9 cm^{-1} in dandelion extract and 1344.3 cm^{-1} in maltodextrin to 1365.4 cm^{-1} in the freeze-dried powder and 1372.7 cm^{-1} in the spray-dried powder. The consistent fingerprint band at around 989–990 cm^{-1} in all samples is attributed to C–H stretching of methylene and methyl groups confirming that the aromatic ring structure of polyphenols remains intact after encapsulation aligning with previous research by Kang *et al.*⁷³ Similar FT-IR shifts for O–H and C–H stretching bands have been reported in earlier microencapsulation studies involving dandelion leaf extract by the spray drying process by Martinic *et al.*⁷⁴ These findings demonstrate that the encapsulation process, along with the drying methods, has a significant effect on the molecular interactions between the tea extract and maltodextrin, with slight differences observed between freeze-dried and spray-dried powders. The variations in vibrational peaks between spray-dried and freeze-dried powder samples could stem from the higher thermal conditions employed during spray drying that causes structural modifications that ultimately affect the oscillatory behaviour of the functional groups. While investigating the sea buckthorn fava bean composite instant powder, similar observations were made by Li *et al.*⁷⁵ for spray and freeze-drying effects on physicochemical properties, bio actives and sensory attributes.

3.5.3 Scanning electron microscopy (SEM). Surface characteristics of encapsulated nanoparticles were identified from freeze and spray drying through scanning electron microscopy (SEM) as shown in Fig. 3. The image clearly indicates that the particle morphology varied between two drying methods. Scanning electron micrographs showed that spray-dried nanoparticles revealed spherical to dented-spherical shapes, (Fig. 3a and b), whereas the freeze-dried nanoparticles showed broken,

flaky, porous structures, and irregular shapes with edges (Fig. 3c and d). The flaky shapes obtained during freeze drying might be ascribed to reduced drying heat and lack of forces that typically fragments frozen liquid into fragmented particles or significantly alters their surface characteristics. Furthermore, during the initial freezing stage, ice crystals form, and as they sublime, they create small pores, which increase the surface area of the particles. This process results in a loose, porous, cake-like structure,⁷⁶ while the spray-dried powder's morphology showed spherical to dented-spherical shapes. The spherical appearance of spray-dried particles resulted from atomization, which promoted the fast evaporation of water owing to the formation of a protective film over the surface of the droplet in the early stages of drying. Similar studies have been reported by Martinic *et al.*⁷⁴ Moreover, the formation of dented structures in the nanoencapsulates may be linked to the rapid moisture evaporation loss and temperature reduction that occurs during the process of spray-drying.¹¹ In a study by Dadi *et al.*,⁴³ similar morphological features were identified in microencapsulated bioactive compounds derived from *Moringa stenopetala* leaf extract, produced through freeze-drying and spray-drying methods.

3.5.4 *In vitro* release. The release behaviour of nano-encapsulated dandelion tea from the wall material was analyzed under simulated gastrointestinal *in vitro* conditions under SGF and SIF. Understanding the mechanisms that control the dispersion of dandelion tea from nano-encapsulated matrices during digestion is essential. This includes examining its response to varying pH levels and its interaction with gastrointestinal enzymes. To evaluate the release kinetics of nano-encapsulated freeze and spray-dried dandelion tea, its concentration in digestive media was measured at specific time intervals, as outlined in Section 3.0. Therefore, the investigation was carried out at pH 2 and 37 °C for 2 hours to simulate digestive conditions, followed by an adjustment to pH 7.5 for 4 hours to replicate the enteric conditions. The release behaviour of dandelion encapsulated tea was affected by properties of the wall material and the effectiveness of encapsulation capacity. As illustrated in Fig. 4, the release of dandelion tea was higher in SIF compared to SGF for both treatments. The relatively lower release in SGF (23.55% for freeze-dried and 20.62% for spray-dried) might be due to lower solubility of maltodextrin under highly acidic conditions such as in gastric fluids at pH 2.0, while it dissolves more readily in neutral to alkaline environments such as intestinal fluids, at pH 6.8–7.5. This leads to a slower release in the stomach and a higher release in intestines. Furthermore, maltodextrin also protected the encapsulates by forming a thick insoluble layer which was also resistant to gastric digestion.⁷⁷ Our findings align with the results of Parvez *et al.*,²⁷ while encapsulating green tea extract using maltodextrin as a wall material. Furthermore, when evaluating the *in vitro* release percentages of freeze dried and spray-dried powders, a significant difference was observed as shown in Table 7. The release profile of dandelion tea freeze-dried powder in the stomach and intestinal phases was recorded as 23.55% \pm 0.92 and 75.76% \pm 1.46 respectively. Meanwhile, the spray-dried powder showed release percentages of 20.62% \pm 1.51 in the



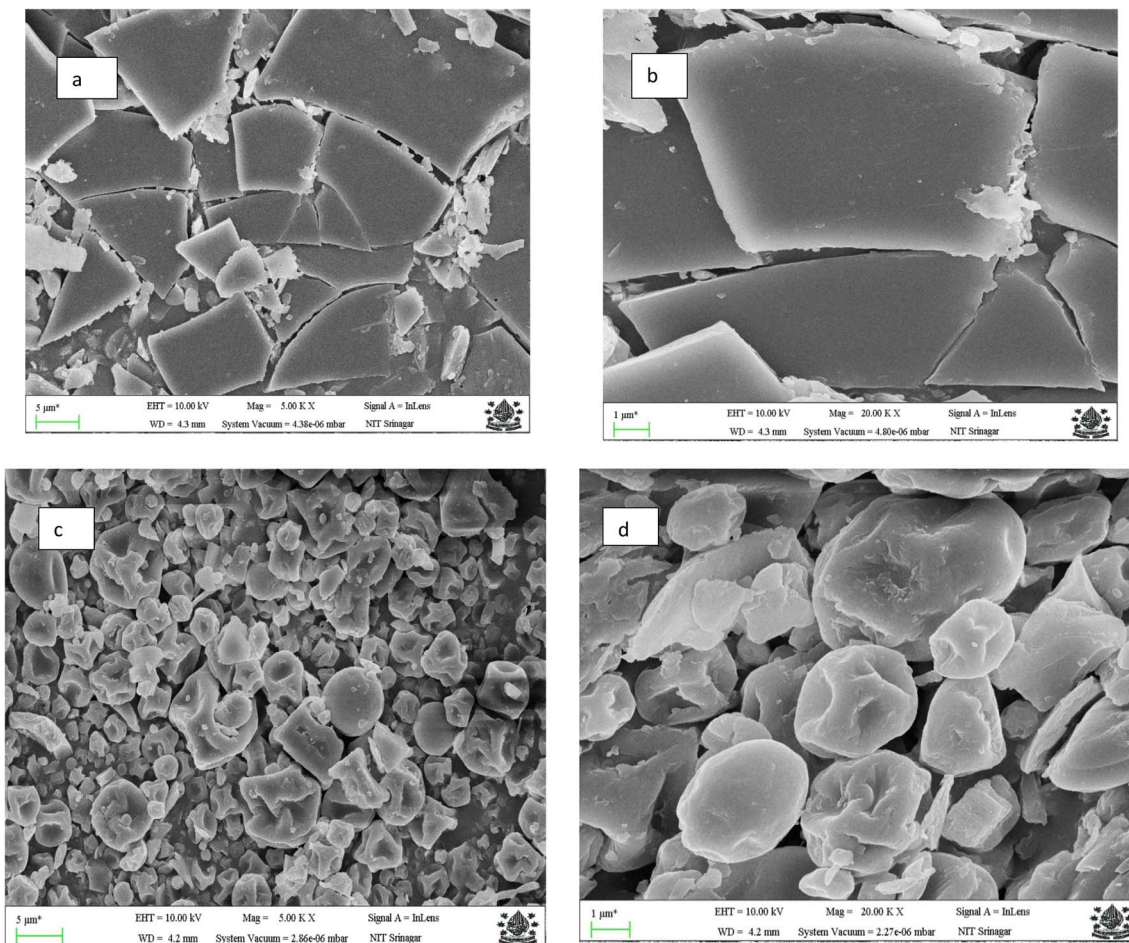


Fig. 3 (a–d) Scanning Electron Microscopy (SEM) images of freeze-dried tea powder (a and b) and spray dried tea powder (c and d).

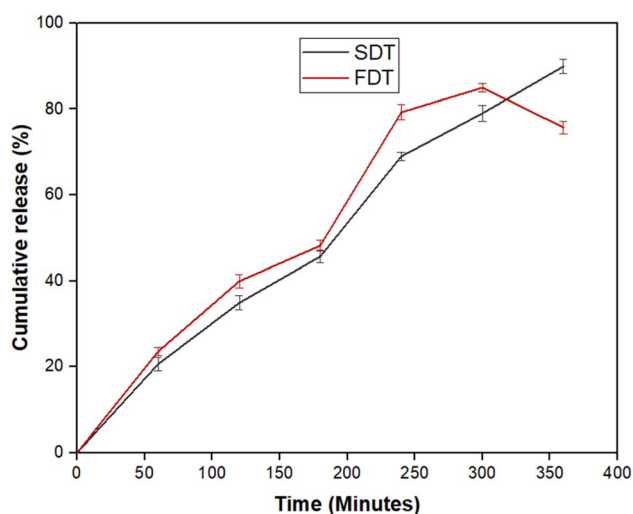


Fig. 4 *In vitro* bioactive release behaviour of freeze dried and spray dried tea nanoparticles in simulated gastric digestion (0–2 h) and simulated intestinal digestion (2–6 h).

stomach and $89.92\% \pm 1.70$ in the intestinal phase, indicating that spray drying resulted in superior retention and a more controlled release of dandelion tea under intestinal conditions.

The release of freeze-dried nanoencapsulates was initially much higher than that of spray-dried nanoencapsulates, followed by a sharp decline as digestion progressed. This rapid release pattern may be attributed to the lower encapsulation efficiency and weaker structural stability of the freeze-dried matrix, which tends to disintegrate quickly under gastrointestinal conditions, allowing bioactive compounds to diffuse out more rapidly in the early stages. In contrast, spray-dried nanoencapsulates exhibited a more gradual and sustained release profile, likely due to the stronger binding capacity of the coating material formed at higher inlet air temperatures during spray drying. Furthermore, the smaller size and globular structure of spray-dried nanoencapsulates contributed to improved retention and a controlled release of dandelion tea, reinforcing the idea that particle size directly influences the delivery of bioactive compounds. Overall, the study demonstrated that nanoencapsulation effectively preserved dandelion tea, enhancing its stability and promoting its release under simulated gastrointestinal conditions. This improved its bioavailability while minimizing degradation. Rosa *et al.*⁷⁸ also observed that the release of encapsulated anthocyanins from blueberry extract was lower in a simulated gastric environment in comparison to under intestinal conditions.



Table 7 Release kinetic model parameters of nanoencapsulated tea powders dried by freeze and spray drying

Sample	Zero order		First order		Higuchi		Hixson–Crowell		Korsmeyer–Peppas		
	K_0	R^2	K_1	R^2	K_H	R^2	K_{HC}	R^2	K_{KP}	R^2	n
Freeze dried	0.265	0.8570	0.005	0.9428	4.288	0.9105	0.001	0.9459	1.712	0.93210	0.667
Spray dried	0.263	0.9852	0.004	0.9562	4.206	0.9157	0.001	0.9784	0.560	0.9927	0.866

3.5.5 Release profile analysis. The release profile analysis of dandelion tea extracted nanoparticles obtained through spray and freeze drying was conducted by modelling the data to various mathematical models, like zero-order, first-order, Higuchi, Hixson-Crowell, and Korsmeyer-Peppas to analyse drug release kinetics. The release kinetic constants (K) and regression coefficient (R^2) are presented in Table 7. Ideally, the core material's release profile should be either zero-order or first-order. In general, the best model for explaining the behaviour of releases from nanoparticles is the zero-order model, as it ensures a consistent and prolonged release, independent of time. Usually, a first-order release pattern occurs when the core material is in solution.⁷⁹

The delivery of the active component is influenced by variations in particle size and surface area, according to the Hixson-Crowell model, while the Higuchi model characterizes the release mechanism as being predominantly regulated by diffusion. The Korsmeyer-Peppas model provided the optimal fit for the present data. The regression coefficient R^2 values obtained by the Korsmeyer-Peppas model for dandelion tea nanoparticles was recorded to be 0.9321 0 for freeze-dried nanoparticles and 0.9927 for spray-dried nanoparticles. This model also aids in characterizing the release mechanism through the diffusion exponent (n). If $n \leq 0.5$, the release follows Fickian diffusion. For values of $n \geq 0.89$, the release mechanism indicates super case II transport through polymeric chain erosion. When n is between 0.45 and 0.89, an anomalous (non-Fickian) release mechanism occurs, involving both diffusion and swelling. The n values for nanoparticles obtained through freeze-dried and spray-dried nanoparticles (0.667–0.866) suggest a non-Fickian diffusion transport mechanism. Similar findings were reported by Ledari *et al.*⁷⁰ during encapsulation of chlorophyll using freeze drying and spray drying techniques.

4. Conclusion

Instant herbal dandelion tea powder was developed by nano-encapsulation of dandelion leaf extracts by optimizing the brewing conditions using Box-Behnken design. Comparative evaluation of spray- and freeze-dried nanoencapsulated powders demonstrated that spray-dried particulates exhibited superior encapsulation efficiency, surface morphology, flowability, and reconstitution behaviour parameters that are critical for practical application in herbal tea formulations. The study revealed that spray-dried nanoparticulates with polyphenolic compounds exhibited superior encapsulation efficiency, surface characteristics, and release behaviour. The release profile closely followed the Korsmeyer-Peppas model,

which exhibited the highest R^2 values across the samples and was therefore identified as the best-fit model for sustained-release formulations. However, the zero-order model also provided an excellent fit for the spray-dried nanoparticulates, further supporting their sustained-release behaviour. These findings indicate that nano-encapsulation of dandelion tea extract with maltodextrin is a promising approach for enhancing its stability under simulated gastrointestinal conditions. In addition to lower energy requirements for industrial-scale processing, enhanced solubility, dispersibility, and stability further support spray drying as the preferred method for producing functional nanoencapsulated dandelion tea powders. The developed product offers an innovative nutraceutical beverage which can be scaled up to the industrial set up. Future studies should explore the incorporation of these encapsulated nanoparticles into herbal tea formulations to evaluate their stability, controlled release properties, and potential health benefits.

Author contributions

Qudsiya Ayaz: writing – original draft, software, formal analysis, data curation, Nadira Anjum: validation, software, Sehrish Mustafa: writing review & editing, Abdul Rouf: supervision, project administration, Imtiyaz Ahmad Zargar: supervision and project administration, and Sajad Mohd Wani: supervision, resources, project administration, investigation.

Conflicts of interest

There are no conflicts to declare.

Data availability

Data will be made available on request.

Acknowledgements

This work has been financially supported by the Department of Biotechnology (DBT), New Delhi. BT/PR45204/NER/95/1931/2022.

References

- 1 G. E. Okpiaifo, B. Dormoy-Smith, B. Kassas and Z. Gao, Perception and demand for healthy snacks/beverages among US consumers vary by product, health benefit, and color, *PLoS One*, 2023, **18**(6), e0287232.



- 2 V. Puri, M. Nagpal, I. Singh, M. Singh, G. A. Dhingra, K. Huanbutta, D. Dheer, A. Sharma and T. Sangnim, A comprehensive review on nutraceuticals: therapy support and formulation challenges, *Nutrients*, 2022, **14**(21), 4637.
- 3 X. Long, S. Ranjitkar, A. Waldstein, H. Wu, Q. Li and Y. Geng, Preliminary exploration of herbal tea products based on traditional knowledge and hypotheses concerning herbal tea selection: a case study in Southwest Guizhou, China, *J. Ethnobiol. Ethnomed.*, 2024, **20**(1), 1.
- 4 M. S. Hosen and B. Madhu, *Health benefits of herbal tea: a review*, Daffodil International University, 2023, vol. 10, pp. 1–10.
- 5 Y. Zhu, W. Gu, R. Tian, C. Li, Y. Ji, T. Li, C. Wei and Z. Chen, Morphological, physiological, and secondary metabolic responses of *Taraxacum officinale* to salt stress, *Plant Physiol. Biochem.*, 2022, **189**, 71–82.
- 6 C. Someswararao and P. P. Srivastav, A novel technology for production of instant tea powder from the existing black tea manufacturing process, *Innovative Food Sci. Emerging Technol.*, 2012, **16**, 143–147.
- 7 V. Kraujalytė, E. Pelvan and C. Alasalvar, Volatile compounds and sensory characteristics of various instant teas produced from black tea, *Food Chem.*, 2016, **194**, 864–872.
- 8 L. M. Sagis, *Microencapsulation and Microspheres for Food Applications*, Academic Press, 2015, 1–550.
- 9 A. Gharsallaoui, G. Roudaut, O. Chambin, A. Voilley and R. Saurel, Applications of spray-drying in microencapsulation of food ingredients: an overview, *Food Res. Int.*, 2007, **40**(9), 1107–1121.
- 10 F. Sansone, T. Mencherini, P. Picerno, M. d'Amore, R. P. Aquino and M. R. Lauro, Maltodextrin/pectin microparticles by spray drying as carrier for nutraceutical extracts, *J. Food Eng.*, 2011, **105**(3), 468–476.
- 11 A. Tolun, Z. Altintas and N. Artik, Microencapsulation of grape polyphenols using maltodextrin and gum arabic as two alternative coating materials: development and characterization, *J. Biotechnol.*, 2016, **239**, 23–33.
- 12 S. Y. Hundre, P. Karthik and C. Anandharamkrishnan, Effect of whey protein isolate and β -cyclodextrin wall systems on stability of microencapsulated vanillin by spray-freeze drying method, *Food Chem.*, 2015, **174**, 16–24.
- 13 L. Yao, X. Liu, Y. Jiang, N. Caffin, B. D'Arcy, R. Singanusong and Y. Xu, Compositional analysis of teas from Australian supermarkets, *Food Chem.*, 2006, **94**(1), 115–122.
- 14 A. Kumaran and R. J. Karunakaran, In vitro antioxidant activities of methanol extracts of five *Phyllanthus* species from India, *LWT-Food Sci. Technol.*, 2007, **40**(2), 344–352.
- 15 I. O. Pfingstgraf, M. Taulescu, R. M. Pop, R. Orăsan, L. Vlase, A. Uifalean and A. E. Părvu, Protective effects of *Taraxacum officinale* L. (dandelion) root extract in experimental acute on chronic liver failure, *Antioxidants*, 2021, **10**(4), 504.
- 16 L. G. L. Gerolis, F. S. Lameiras, K. Krambrock and M. J. Neves, Effect of gamma radiation on antioxidant capacity of green tea, yerba mate, and chamomile tea as evaluated by different methods, *Radiat. Phys. Chem.*, 2017, **130**, 177–185.
- 17 G. W. Shuen, L. Y. Yi, T. S. Ying, G. C. Y. Von, Y. A. B. Yusof and P. L. Phing, Effects of drying methods on the physicochemical properties and antioxidant capacity of Kuini powder, *Braz. J. Food Technol.*, 2021, **24**, e2020086.
- 18 N. Jinapong, M. Suphantharika and P. Jamnong, Production of instant soymilk powders by ultrafiltration, spray drying and fluidized bed agglomeration, *J. Food Eng.*, 2008, **84**(2), 194–205.
- 19 J. A. Zokti, B. Sham Baharin, A. S. Mohammed and F. Abas, Green tea leaves extract: microencapsulation, physicochemical and storage stability study, *mol.*, 2016, **21**(8), 940.
- 20 J. Mujica-Álvarez, O. Gil-Castell, P. A. Barra, A. Ribes-Greus, R. Bustos, M. Faccini and S. Matiacevich, Encapsulation of vitamins A and E as spray-dried additives for the feed industry, *mol.*, 2020, **25**(6), 1357.
- 21 S. Saikia, N. K. Mahnot and C. L. Mahanta, Optimisation of phenolic extraction from *Averrhoa carambola* pomace by response surface methodology and its microencapsulation by spray and freeze drying, *Food Chem.*, 2015, **171**, 144–152.
- 22 P. Filippou, S. T. Mitrouli and P. Vareltsis, Sequential membrane filtration to recover polyphenols and organic acids from red wine lees: the antioxidant properties of the spray-dried concentrate, *Membr.*, 2022, **12**, 353.
- 23 V. Sanna, G. Caria and A. Mariani, Effect of lipid nanoparticles containing fatty alcohols having different chain length on the ex vivo skin permeability of econazole nitrate, *Powder Technol.*, 2010, **201**(1), 32–36.
- 24 R. Rashid, S. M. Wani, S. Manzoor, F. A. Masoodi and A. Altaf, Nanoencapsulation of pomegranate peel extract using maltodextrin and whey protein isolate: characterisation, release behaviour and antioxidant potential during simulated *in vitro* digestion, *Food Biosci.*, 2022, **50**, 102135.
- 25 R. Pulicharla, C. Marques, R. K. Das, T. Rouissi and S. K. Brar, Encapsulation and release studies of strawberry polyphenols in biodegradable chitosan nanoformulation, *Int. J. Biol. Macromol.*, 2016, **88**, 171–178.
- 26 J. Li and Z. Guo, Concurrent extraction and transformation of bioactive phenolic compounds from rapeseed meal using pressurized solvent extraction system, *Ind. Crops Prod.*, 2016, **94**, 152–159.
- 27 S. Parvez, I. A. Wani and F. A. Masoodi, Extraction optimization of green tea beverage (Noon Chai) for yield, polyphenols and caffeine using response surface methodology, *Arab. J. Sci. Eng.*, 2021, **46**, 1–13.
- 28 A. Mokrani and K. Madani, Effect of solvent, time and temperature on the extraction of phenolic compounds and antioxidant capacity of peach (*Prunus persica* L.) fruit, *Sep. Purif. Technol.*, 2016, **162**, 68–76.
- 29 K. N. Prasad, F. A. Hassan, B. Yang, K. W. Kong, R. N. Ramanan, A. Azlan and A. Ismail, Response surface optimisation for the extraction of phenolic compounds and antioxidant capacities of underutilised *Mangifera pajang* Kosterm. peels, *Food Chem.*, 2011, **128**(4), 1121–1127.



- 30 J. Liu, C. Li, G. Ding and W. Quan, Artificial intelligence assisted ultrasonic extraction of total flavonoids from *Rosa sterilis*, *Molecules*, 2021, **26**(13), 3835.
- 31 L. Wang, H. Zhang, M. Xie, J. Wan, J. Li, S. Yang and Y. Xiong, Optimization of brewing process vine tea and flavor analysis of different brewing processes, *J. Food Biochem.*, 2024, **48**(1), 8858457.
- 32 A. D. Sousa, A. I. V. Maia, T. H. S. Rodrigues, K. M. Canuto, P. R. V. Ribeiro, R. D. C. A. Pereira and E. S. de Brito, Ultrasound-assisted and pressurized liquid extraction of phenolic compounds from *Phyllanthus amarus* and its composition evaluation by UPLC-QTOF, *Ind. Crops Prod.*, 2016, **79**, 91–103.
- 33 S. Insang, I. Kijpatanasilp, S. Jafari and K. Assatarakul, Ultrasound-assisted extraction of functional compound from mulberry (*Morus alba* L.) leaf using response surface methodology and effect of microencapsulation by spray drying on quality of optimized extract, *Ultrason. Sonochem.*, 2022, **82**, 105806.
- 34 Y. Liu, L. Luo, C. Liao, L. Chen, J. Wang and L. Zeng, Effects of brewing conditions on the phytochemical composition, sensory qualities and antioxidant activity of green tea infusion: a study using response surface methodology, *Food Chem.*, 2018, **269**, 24–34.
- 35 L. S. Lee, N. Lee, Y. H. Kim, C. H. Lee, S. P. Hong, Y. W. Jeon and Y. E. Kim, Optimization of ultrasonic extraction of phenolic antioxidants from green tea using response surface methodology, *Molecules*, 2013, **18**(11), 13530–13545.
- 36 R. Wati, S. Sampanvejsobha and N. Punbusayakul, Effect of extraction conditions on Assam green tea, *Agric. Sci. J.*, 2009, **40**, 47–50.
- 37 A. P. Tambunan, A. Bahtiar and R. R. Tjandrawinata, Influence of extraction parameters on the yield, phytochemical, TLC-densitometric quantification of quercetin, and LC-MS profile, and how to standardize different batches for long term from *Ageratum conyzoides* L. leaves, *Pharmacogn. J.*, 2017, **9**(6), 767–774.
- 38 H. N. T. Pham, V. T. Nguyen, Q. V. Vuong, M. C. Bowyer and C. J. Scarlett, Effect of extraction solvents and drying methods on the physicochemical and antioxidant properties of *Helicteres hirsuta* Lour. leaves, *Technol.*, 2015, **3**(4), 285–301.
- 39 S. A. Mahdavi, S. M. Jafari, E. Assadpoor and D. Dehnad, Microencapsulation optimization of natural anthocyanins with maltodextrin, gum Arabic and gelatin, *Int. J. Biol. Macromol.*, 2016, **85**, 379–385.
- 40 Z. Abdullah, F. S. Taip, S. M. M. Kamal and R. Z. A. Rahman, Nonlinear model-based inferential control of moisture content of spray dried coconut milk, *Foods*, 2020, **9**(9), 1177.
- 41 L. S. Kuck and C. P. Z. Norena, Microencapsulation of grape (*Vitis labrusca* var. *Bordo*) skin phenolic extract using gum Arabic, polydextrose, and partially hydrolyzed guar gum as encapsulating agents, *Food Chem.*, 2016, **194**, 569–576.
- 42 R. V. D. B. Fernandes, S. V. Borges and D. A. Botrel, Influence of spray drying operating conditions on microencapsulated rosemary essential oil properties, *Food Sci. Technol.*, 2013, **33**, 171–178.
- 43 D. W. Dadi, S. A. Emire, A. D. Hagos and J. B. Eun, Physical and functional properties, digestibility, and storage stability of spray- and freeze-dried microencapsulated bioactive products from *Moringa stenopetala* leaves extract, *Ind. Crops Prod.*, 2020, **156**, 112891.
- 44 H. Mitra, H. A. Pushpadass, M. E. E. Franklin, R. K. Ambrose, C. Ghoroi and S. N. Battula, Influence of moisture content on the flow properties of basundi mix, *Powder Technol.*, 2017, **312**, 133–143.
- 45 S. Parvez, I. A. Wani and F. A. Masoodi, Extraction optimization of green tea beverage (Noon Chai) for yield, polyphenols and caffeine using response surface methodology, *Arab. J. Sci. Eng.*, 2022, 1–13.
- 46 I. Bashir, S. M. Wani, A. A. Bhat, A. A. Khan, S. Z. Hussain, S. A. Ganai and N. Anjum, Effect of freeze drying and spray drying on physical properties, morphology and *in vitro* release kinetics of vitamin D3 nanoparticles, *Powder Technol.*, 2024, **432**, 119164.
- 47 R. V. Tonon, C. Brabet and M. D. Hubinger, Influence of process conditions on the physicochemical properties of açai (*Euterpe oleraceae* Mart.) powder produced by spray drying, *J. Food Eng.*, 2008, **88**(3), 411–418.
- 48 L. A. Egas-Astudillo, N. Martínez-Navarrete and M. D. M. Camacho, Quality of a powdered grapefruit product formulated with biopolymers obtained by freeze-drying and spray-drying, *J. Food Sci.*, 2021, **86**(6), 2255–2263.
- 49 M. C. Karam, J. Petit, D. Zimmer, E. B. Djantou and J. Scher, Effects of drying and grinding in production of fruit and vegetable powders: A review, *J. Food Eng.*, 2016, **188**, 32–49.
- 50 K. Muzaffar, B. N. Dar and P. Kumar, Assessment of nutritional, physicochemical, antioxidant, structural and rheological properties of spray dried tamarind pulp powder, *J. Food Meas. Charact.*, 2017, **11**, 746–757.
- 51 J. J. Fitzpatrick, K. Barry, P. S. M. Cerqueira, T. Iqbal, J. O'Neill and Y. H. Roos, Effect of composition and storage conditions on the flowability of dairy powders, *Int. Dairy J.*, 2007, **17**(4), 383–392.
- 52 Y. Ma, J. Gao, W. Jia, Y. Liu, L. Zhang, Q. Yang and Y. Wang, A comparison of spray-drying and freeze-drying for the production of stable silybin nanosuspensions, *J. Nanosci. Nanotechnol.*, 2020, **20**(6), 3598–3603.
- 53 G. Caliskan and S. N. Dirim, The effect of different drying processes and the amounts of maltodextrin addition on the powder properties of sumac extract powders, *Powder Technol.*, 2016, **287**, 308–314.
- 54 H. Aryaee, P. Ariaii, D. Zare, S. Mirdamadi and S. N. Raeisi, Evaluation of the physicochemical characteristics of a blend fruit juice powder mixed with *Lactiplantibacillus plantarum*: A comparison of spray drying and freeze drying, *J. Food Process. Preserv.*, 2023, **1**, 5597647.
- 55 Q. Chen, F. Zhong, J. Wen, D. McGillivray and S. Y. Quek, Properties and stability of spray-dried and freeze-dried microcapsules co-encapsulated with fish oil, phytoesterols, and limonene, *Dry. Technol.*, 2013, **31**(6), 707–716.
- 56 X. Xin, S. Essien, K. Dell, M. W. Woo and S. Baroutian, Effects of spray-drying and freeze-drying on bioactive and



- volatile compounds of smoke powder food flavouring, *Food Bioprocess Technol.*, 2022, **15**, 785–794.
- 57 M. E. da Silva Júnior, M. V. R. L. Araújo, A. C. S. Martins, M. dos Santos Lima, F. L. H. Da Silva, A. Converti and M. I. S. Maciel, Microencapsulation by spray-drying and freeze-drying of extract of phenolic compounds obtained from ciriguela peel, *Sci. Rep.*, 2023, **13**(1), 15222.
- 58 P. Varelziz, D. Fotiou, V. Papatheologou, S. Kyroglou, E. Tsachouridou and A. M. Goula, Optimized solid-liquid separation of phenolics from lavender waste and properties of the dried extracts, *Sep.*, 2024, **11**(3), 67.
- 59 P. Varelziz, A. Stergiou, K. Kalinderi and M. Chamilaki, Antioxidant potential of spray- and freeze-dried extract from oregano processing wastes, using an optimized ultrasound-assisted method, *Foods*, 2023, **12**(13), 2628.
- 60 W. F. Gomes, F. R. França, M. Denadai, J. K. Andrade, E. M. da Silva Oliveira, E. S. de Brito, S. Rodrigues and N. Narain, Effect of freeze- and spray-drying on physico-chemical characteristics, phenolic compounds and antioxidant activity of papaya pulp, *J. Food Sci. Technol.*, 2018, **55**(6), 2095–2102.
- 61 C. P. Liang, C. H. Chang, C. C. Liang, K. Y. Hung and C. W. Hsieh, In vitro antioxidant activities, free radical scavenging capacity, and tyrosinase inhibitory of flavonoid compounds and ferulic acid from *Spiranthes sinensis* (Pers.) Ames, *Molecules*, 2014, (19), 4681–4694.
- 62 I. P. Turkiewicz, A. Wojdyło, K. Tkacz, K. Lech, A. Michalska-Ciechanowska and P. Nowicka, The influence of different carrier agents and drying techniques on physical and chemical characterization of Japanese quince (*Chaenomeles japonica*) microencapsulation powder, *Food Chem.*, 2020, (323), 126830.
- 63 F. H. Brishti, S. Y. Chay, K. Muhammad, M. R. Ismail-Fitry, M. Zarei, S. Karthikeyan and N. Saari, Effects of drying techniques on the physicochemical, functional, thermal, structural and rheological properties of mung bean (*Vigna radiata*) protein isolate powder, *Food Res. Int.*, 2020, **138**, 109783.
- 64 W. Chen, H. T. Chiu, Z. Feng, E. Maes and L. Serventi, Effect of spray-drying and freeze-drying on the composition, physical properties, and sensory quality of pea processing water (*Liluva*), *Foods*, 2021, **10**(6), 1401.
- 65 S. Ahmadian, R. E. Kenari, Z. R. Amiri, F. Sohbatzadeh and M. H. H. Khodaparast, Fabrication of double nano-emulsions loaded with hyssop (*Hyssopus officinalis* L.) extract stabilized with soy protein isolate alone and combined with chia seed gum in controlling the oxidative stability of canola oil, *Food Chem.*, 2024, **430**, 137093.
- 66 Y. Ma, S. Chen, W. Liao, L. Zhang, J. Liu and Y. Gao, Formation, physicochemical stability, and redispersibility of curcumin-loaded rhamnolipid nanoparticles using the pH-driven method, *J. Agric. Food Chem.*, 2020, **68**(27), 7103–7111.
- 67 D. E. Walton, The morphology of spray-dried particles: A qualitative view, *Dry. Technol.*, 2000, **18**(9), 1943–1986.
- 68 A. Seyfoddin and R. Al-Kassas, Development of solid lipid nanoparticles and nanostructured lipid carriers for improving ocular delivery of acyclovir, *Drug Dev. Ind. Pharm.*, 2013, **39**(4), 508–519.
- 69 I. E. Agarry, Z. Wang, T. Cai, J. Kan and K. Chen, Chlorophyll encapsulation by complex coacervation and vibration nozzle technology: Characterization and stability study, *Innov. Food Sci. Emerg. Technol.*, 2022, **78**, 103017.
- 70 S. A. Ledari, J. M. Milani, S. A. Shahidi and A. Golkar, Comparative analysis of freeze drying and spray drying methods for encapsulation of chlorophyll with maltodextrin and whey protein isolate, *Food Chem. X*, 2024, **21**, 101156.
- 71 H. Tiernan, B. Byrne and S. G. Kazarian, ATR-FTIR spectroscopy and spectroscopic imaging for the analysis of biopharmaceuticals, *Spectrochim. Acta A Mol. Biomol. Spectrosc.*, 2020, **241**, 118636.
- 72 T. Arumugham, R. Krishnamoorthy, J. AlYammahi, S. W. Hasan and F. Banat, Spray-dried date fruit extract with a maltodextrin/gum arabic binary blend carrier agent system: Process optimization and product quality, *Int. J. Biol. Macromol.*, 2023, **238**, 124340.
- 73 Y. R. Kang, Y. K. Lee, Y. J. Kim and Y. H. Chang, Characterization and storage stability of chlorophylls microencapsulated in different combinations of gum arabic and maltodextrin, *Food Chem.*, 2019, **272**, 337–346.
- 74 A. Martinić, A. Kalušević, S. Lević, V. Nedović, A. Vojvodić Cebin, S. Karlović, I. Špoljarić, G. Mršić, K. Žižek and D. Komes, Microencapsulation of dandelion (*Taraxacum officinale* L.) leaf extract by spray drying, *Food Technol. Biotechnol.*, 2022, **60**(2), 237–252.
- 75 S. Li, X. Fu, J. Wen, L. Jiang, L. Shao, Y. Du and C. Shan, Characterization of physicochemical properties, bioactivities, and sensory attributes of sea buckthorn-fava bean composite instant powder: Spray-drying versus freeze-drying coupled with carriers, *Foods*, 2024, **13**(23), 3944.
- 76 R. A. Kurniasih, E. N. Dewi and L. Purnamayati, Effect of different coating materials on the characteristics of chlorophyll microcapsules from *Caulerpa racemosa*, *IOP Conf. Ser. Earth Environ. Sci.*, 2018, **116**(1), 012030.
- 77 K. Yadav, R. K. Bajaj, S. Mandal and B. Mann, Encapsulation of grape seed extract phenolics using whey protein concentrate, maltodextrin and gum arabic blends, *J. Food Sci. Technol.*, 2020, **57**, 426–434.
- 78 J. R. da Rosa, G. C. C. Weis, K. I. B. Moro, S. S. Robalo, C. E. Assmann, L. P. P. da Silva, E. I. Muller, C. D. B. da Silva, C. R. de Menezes and C. S. da Rosa, Effect of wall materials and storage temperature on anthocyanin stability of microencapsulated blueberry extract, *LWT*, 2021, **142**, 111027.
- 79 A. M. Ribeiro, M. Shahgol, B. N. Estevinho and F. Rocha, Microencapsulation of vitamin A by spray-drying, using binary and ternary blends of gum arabic, starch, and maltodextrin, *Food Hydrocoll.*, 2020, **108**, 106029.

